ELSEVIER

Influence of nanosized Ni(OH)$_2$ addition on the electrochemical performance of nickel hydroxide electrode

Xiaohong Liu*, Lan Yu

College of Chemistry and Molecular Sciences, Wuhan University, Wuhan 430072, PR China

Abstract

Nanosized cathode material Ni(OH)$_2$ for alkaline batteries was prepared by converting the precursor of NiC$_2$O$_4$·2H$_2$O in KOH water solution which contained Tween-80, and the precursor was obtained via the reaction between Ni(NO$_3$)$_2$·6H$_2$O and H$_2$C$_2$O$_4$·2H$_2$O in ethanol solvent. The products were characterized using X-ray diffraction (XRD), infrared absorption spectroscopy (IR), and transmission electron microscopy (TEM). The results showed that the as-prepared Ni(OH)$_2$ sample by this method is β(II)-type phase and its shape is spherical with the particle size from 5 to 35 nm. The electrochemical studies revealed that the 10% addition of nanosized Ni(OH)$_2$ to common microsized spherical Ni(OH)$_2$ can improve the electrochemical performance of the Ni(OH)$_2$ electrode. There exists approximately a 10% improvement in the utilization of the active material of the Ni(OH)$_2$ electrode with 10% nannosized Ni(OH)$_2$ addition in comparison with microsized spherical Ni(OH)$_2$ electrode. Nanosized Ni(OH)$_2$ may be a promising cathodic active material for alkaline rechargeable batteries.
© 2003 Elsevier B.V. All rights reserved.

1. Introduction

Alkaline rechargeable batteries such as Ni–metal hydride (Ni–MH), nickel–cadmium (Ni–Cd) and nickel–iron (Ni–Fe) are widely applied to today's market covering domains ranging from power tools to portable electronics and electric vehicle. Nickel hydroxide is the active material for cathode of these batteries. The development of nickel hydroxide has gone through from traditionally agglomerated nickel hydroxide to spherical β-Ni(OH)$_2$ [1]. Traditionally, the theoretical capacity of nickel hydroxide electrode is believed to be 289 mAh/g if the electrode reaction during charge–discharge process involves one-electron transfer. But in high power applications such as electric vehicles, it is limited by the discharge–charge rate which determines the vehicle acceleration and recharge rate of the Ni–MH battery [2].

For further battery applications, single-phase nickel hydroxide products with good crystallinity, homogeneity, uniform morphology with submicrometer particle size distribution, and high surface area are necessary. It has been reported that nickel hydroxide with a smaller crystalline size shows better charge–discharge cyclic characteristics and a higher proton diffusion coefficient [3]. US Nanocorp, Inc. (USN) has developed an aqueous solution reaction (ASR) technique scalable for high volume production of nanostructured nickel hydroxide for a wide range of applications, it is expected to yield at least a 20% improvement in cathode energy content [4]. The capacity of the Ni(OH)$_2$ electrode can be increased by about 14% when the electrode was prepared by mixing 8 wt.% nano-phase Ni(OH)$_2$ with spherical Ni(OH)$_2$ [5].

In this paper, nanosized Ni(OH)$_2$ powder was prepared by a so-called precipitate-transformation method and the precursor was synthesized by direct precipitation method in organic solvent with nickel nitrate and oxalic acid. The precursor and the final product have been characterized by X-ray diffraction (XRD), infrared spectrometry (IR), and transmission electron microscopy (TEM). Compared with microsized spherical Ni(OH)$_2$ electrode, the electrochemical properties of the Ni(OH)$_2$ electrode with 10% nannosized

---

* Corresponding author. Present address: Technical Center, Shenzhen-BAK Battery Co. Ltd., No. 4 Building, Lihe Industrial Zone, Shiyan, Bao'an, Shenzhen 518108, PR China. Fax: +86-755-27653006.
E-mail addresses: xiaoling0601@sina.com, liuyuer@gsmail.whu.edu.cn (X. Liu).

$Ni(OH)_2$ addition were studied and, moreover, the influence of nanosized $Ni(OH)_2$ addition on the electrochemical performance of nickel hydroxide electrode was discussed.

2. Experimental

Analytical pure $Ni(NO_3)_2 \cdot 6H_2O$ (nickel nitrate) and $H_2C_2O_4 \cdot 2H_2O$ (oxalic acid) with concentrations of 0.1 M, respectively, were dissolved in ethanol solvent. In the course of magnetically stirred $Ni(NO_3)_2 \cdot 6H_2O$ solution, the same concentration of $H_2C_2O_4 \cdot 2H_2O$ solution was added as precipitator little by little. A kind of light-blue sediment was formed. The above experiment was performed two groups: one group for the subsequent preparation of $Ni(OH)_2$ and another for getting the precursor in order to be characterized by X-ray diffraction and infrared spectrometry. The precipitate obtained by the former group was converted to a $Ni(OH)_2$ precipitate in KOH water solution which contained a small amount of Tween-80. The reaction system was kept at 60 °C and stirred constantly for 6 h. Finally, the $Ni(OH)_2$ precipitate was filtered, rinsed with distilled water, and oven-dried at 60 °C. Another precipitate obtained by the latter group was filtered, ethanol was used to wash the precipitate until the filtered solution was colorless. The washed precipitate was dried in air at 80 °C to get a kind of light-blue precursor.

The XRD powder patterns of the samples were carried out with a Shimadzu XRD 6000 diffractometer. Cu Kα radiation ($\lambda = 1.5418$ Å) operated at 40 kV and 40 mA was used. The scan speed was 4°/min in 2θ. The FT-IR of the precursor was measured on Thermo Nicolet Avatar 360 FT-IR instrument with KBr pellets from 4000 to 400 cm^{-1}. The transmission electron microscope image was performed by means of a JEOL JEM-100cx II microscope. Before observation, the sample was ultrasonically dispersed in ethanol.

Electrochemical properties tests were carried out as follows. Nickel hydroxide powder with 10 wt.% nannosized $Ni(OH)_2$ addition (or microsized spherical β-$Ni(OH)_2$ powder), graphite and polytetrafluoroethylene (PTFE) binder were mixed completely in a weight ratio of 85:10:5, and pressed into a pellet. The pellet was mounted onto a foam nickel for a cathode and dried at 120 °C for 24 h.

Charge–discharge measurements were performed using one nickel hydroxide electrode coupling with a large area platinum sheet electrode. And the electrolyte consisted of 6 mol l^{-1} KOH and 15 g l^{-1} LiOH was used. A Hg/HgO (6 mol l^{-1} KOH + 15 g l^{-1} LiOH) electrode was employed as the reference electrode. Charge–discharge were performed at a rate of 0.2 C, the terminate voltage of discharge is 0.1 V versus Hg/HgO.

Cyclic voltammetric (CV) experiments were performed by means of a CHI660A Electrochemical Workstation (USA), and a three-electrode system with a Hg/HgO reference electrode and a platinum sheet counter electrode with a large area.

3. Results and discussion

3.1. Characterization of the as-synthesized precursor

Fig. 1 shows the XRD pattern of the as-synthesized precursor that was obtained by the reaction between $Ni(NO_3)_2 \cdot 6H_2O$ and $H_2C_2O_4 \cdot 2H_2O$ in ethanol solvent. Its diffraction peak is quite consistent with the standard JCPDS card of $NiC_2O_4 \cdot 2H_2O$. The precursor was confirmed to be pure phase $NiC_2O_4 \cdot 2H_2O$. The average particle size of the precursor of $NiC_2O_4 \cdot 2H_2O$ is about 9 nm, using the Scherrer formula [6] by calculating with line-width method. The reaction is as follows:

$$Ni^{2+} + C_2O_4^{2-} + 2H_2O \rightarrow NiC_2O_4 \cdot 2H_2O \downarrow \qquad (1)$$
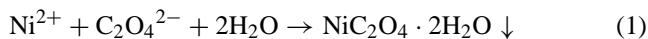
Its structure is as follows [7]:

$$(2)$$

The IR spectrum of the as-synthesized precursor is illustrated in Fig. 2. The frequency values and the assignments of the peaks observed for the precursor of $NiC_2O_4 \cdot 2H_2O$ are listed in Table 1 [7].

3.2. Characterization of nanosized Ni(OH)$_2$

The powder XRD pattern of the as-prepared $Ni(OH)_2$ is shown in Fig. 3. All the reflectance peaks can be indexed as the hexagonal phase of $Ni(OH)_2$ by comparison with the data of the JCPDS file No. 14-0117, which indicated that the crystalline state of the sample is typically β(II)-type $Ni(OH)_2$ phase. The qualitatively large peak widths indicate that the crystalline size is very small. According to
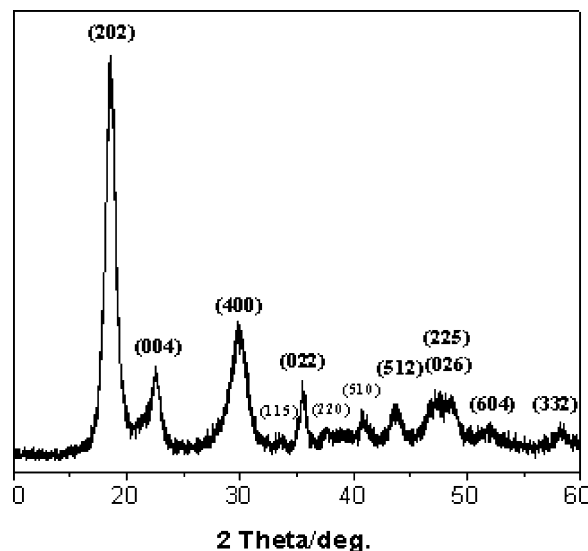

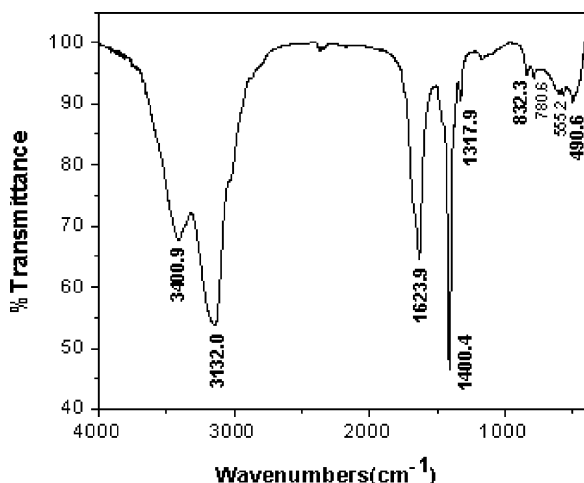Fig. 1. XRD pattern of the as-synthesized precursor.

Fig. 2. IR spectrum of the as-synthesized precursor.

Table 1
Frequencies and band assignments in $NiC_2O_4 \cdot 2H_2O$ precursor

Frequencies (cm^{-1})	Assignment
3400.9	$\nu_{as}(H_2O)$
3132.0	$\nu_s(H_2O)$
1623.9	$\nu_{as}(C=O)$
1400.4	$\nu_s(C–O) + \nu(C–C)$
1317.9	$\nu_s(C–O) + \delta(O–C=O)$
832.3	$\nu_s(C–O) + \delta(O–C=O)$
780.6	$\delta(O–C=O) + \nu(Ni–O)$
555.2	$\nu(Ni–O) + \nu(C–C)$
490.6	$\nu(N–O)$

Scherrer's equation [6], the crystal size of the β-Ni(OH)$_2$ crystals is, respectively, 12 and 7.9 nm as calculated from the (1 0 0) and the (1 0 1) crystal face. The microsized spherical Ni(OH)$_2$ powder used in the experiments is also β(II) phase, and its average particle size is about 8–12 μm. TEM image of the final product is shown in Fig. 4. The resultant product is monolithic, spherical particles with the particle
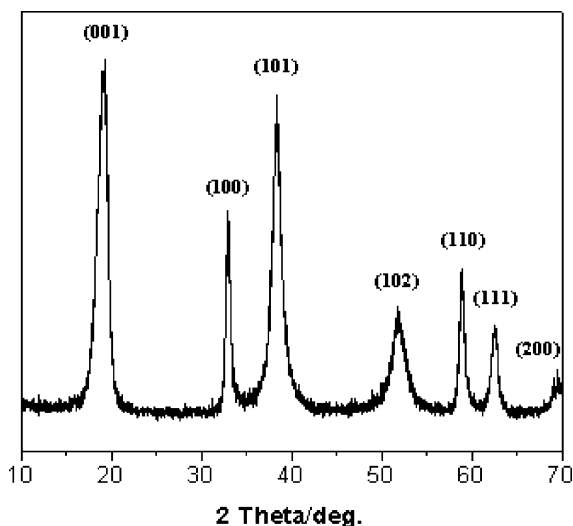
Fig. 3. XRD pattern of Ni(OH)$_2$ powders.
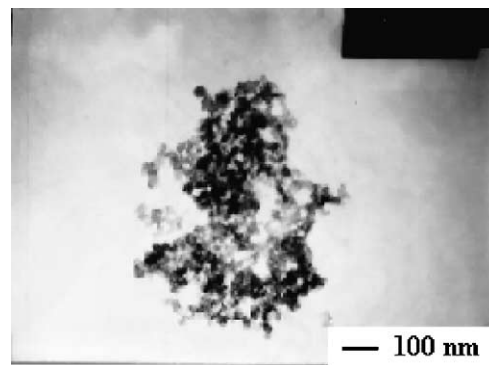
Fig. 4. TEM image of Ni(OH)$_2$ powders.

size from 5 to 35 nm. Coincident with its strong peaks' intensities in XRD pattern, its TEM investigation showed that it is in good crystallinity.

3.3. The weak agglomeration reason of nanosized Ni(OH)$_2$

On the basis of the experiment facts, the reasons helping to understand the weak agglomeration of nanosized Ni(OH)$_2$ particles in this method are as follows.

In the conventional chemical method of usually synthesizing the precursor in water solution, the precursor forms long chains through hydrogen bonds between crystalline water and easily produces agglomeration during subsequent process [8]. However, in this method, the precursor of NiC$_2$O$_4 \cdot$2H$_2$O is synthesized in organic solvent, ethanol chemically and physically absorbed on the surface of the precursor can prevent the formation of the particle chains by hydrogen bonging of adjacent particles, thus bringing on the weak agglomeration or the "soft" agglomeration [9]. Another possible reason for the weak agglomeration formation is that the surfactant Tween-80 used in KOH water solution can prevent the newly produced Ni(OH)$_2$ crystals from growing and aggregating. The weak agglomeration of the as-prepared nanosized Ni(OH)$_2$ particles is ascribed to the above two reasons.

3.4. Cyclic voltammetric measurements

The first cyclic voltammograms of microsized spherical Ni(OH)$_2$ electrode and the Ni(OH)$_2$ electrode with 10% nanosized Ni(OH)$_2$ addition are given in Fig. 5, and the cyclic voltammograms from second to tenth are shown in Figs. 6 and 7, respectively. As seen from Figs. 5–7, before activation, viz. the first cycle, the cathodic and the anodic peak current of the Ni(OH)$_2$ electrode with 10% nanosized Ni(OH)$_2$ addition are much higher than those of microsized Ni(OH)$_2$ electrode and keep higher in the circle from second to tenth, which indicates nanosized Ni(OH)$_2$ added to microsized Ni(OH)$_2$ can improve the electrochemical reactivity and enhance activation of Ni(OH)$_2$ electrode and the
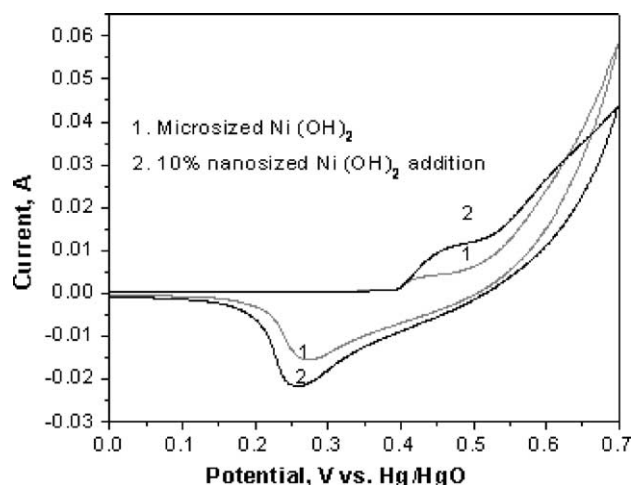
Fig. 5. The first cyclic voltammograms of Ni(OH)$_2$ electrode; scan rate: 2 mV/s.
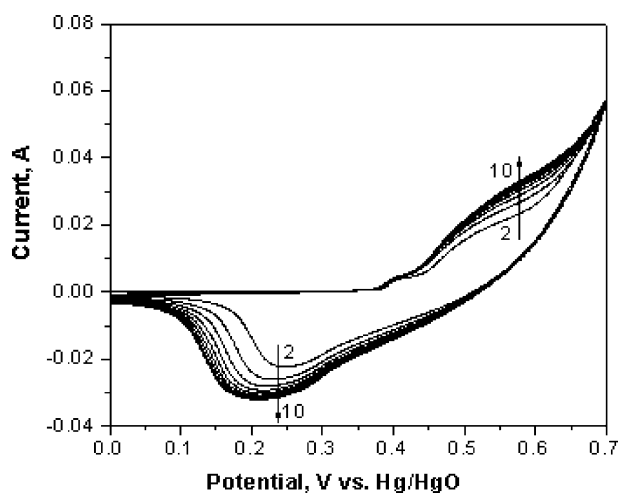

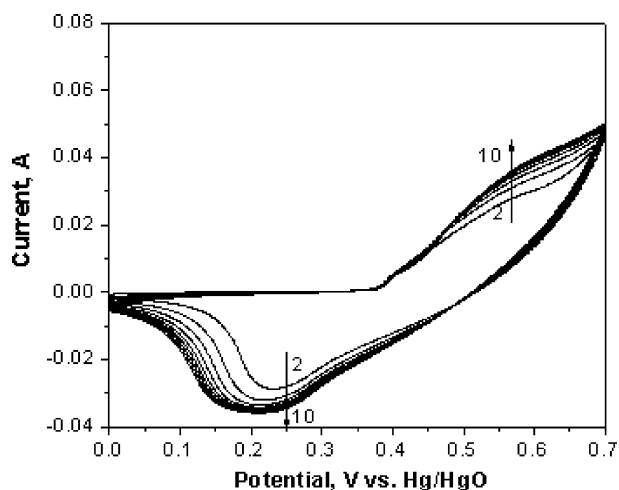Fig. 6. Cyclic voltammograms of microsized Ni(OH)$_2$ electrode (circle number from 2 to 10); scan rate: 2 mV/s.

Fig. 7. Cyclic voltammograms of the Ni(OH)$_2$ electrode with 10% nano-sized Ni(OH)$_2$ addition (circle number from 2 to 10); scan rate: 2 mV/s.
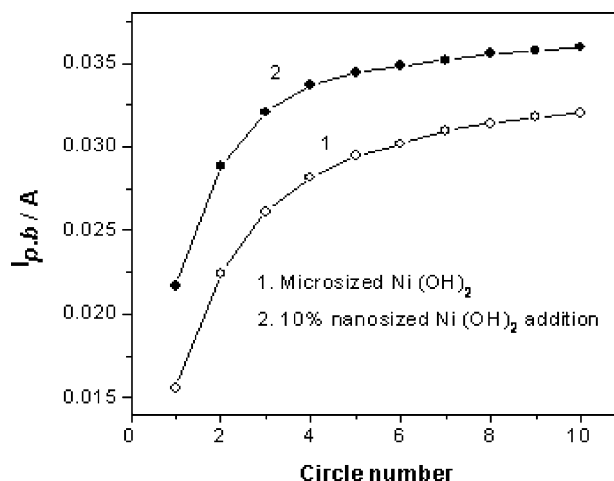

Fig. 8. The variation of $I_{p.b}$ as a function of circle number.

Ni(OH)$_2$ electrode with 10% nanosized Ni(OH)$_2$ addition will has a greater discharge capacity.

It can be seen from Figs. 6 and 7 that the potential positions of the oxidation and reduction peaks of the Ni(OH)$_2$ electrode with 10% nanosized Ni(OH)$_2$ addition do not nearly change with increasing cycles in comparison with those of microsized spherical Ni(OH)$_2$ electrode and the intensity of oxidation and reduction peaks of the Ni(OH)$_2$ electrode with 10% nanosized Ni(OH)$_2$ addition increases gradually with increasing cycles. Therefore, it can be believed that, be the same as microsized spherical Ni(OH)$_2$ electrode, the Ni(OH)$_2$ electrode with 10% nanosized Ni(OH)$_2$ addition has a stable cycle and don't occur the change of structure during charge–discharge process.

Fig. 8 shows the plot of the cathodic peak current $I_{p.b}$ versus circle number. As shown in Fig. 8, the slope of the former segment in curve 2 is greater than that of the former segment in curve 1, and the slope of the latter segment in curve 2 is lower than that of the latter segment in curve 1. These results show that the Ni(OH)$_2$ electrode with 10% nanosized Ni(OH)$_2$ addition has a faster activation and better cyclic stability, and also indicate that it has smaller polarization during the electrochemical redox process.

3.5. The addition performance of nanosized Ni(OH)$_2$ in electrode

Fig. 9 shows the discharge curves of microsized spherical Ni(OH)$_2$ electrode and the Ni(OH)$_2$ electrode with 10% nanosized Ni(OH)$_2$ addition at a rate of 0.2 C. As seen from Fig. 9, the discharging capacity of the Ni(OH)$_2$ electrode with 10% nanosized Ni(OH)$_2$ addition is markedly higher than that of microsized Ni(OH)$_2$ electrode, namely 235 mAh/g versus 214 mAh/g, which reveals that much more active material can be utilized during discharge process in the Ni(OH)$_2$ electrode with 10% nanosized Ni(OH)$_2$ addition. In addition, compared with microsized Ni(OH)$_2$ electrode, the Ni(OH)$_2$ electrode with 10% nanosized
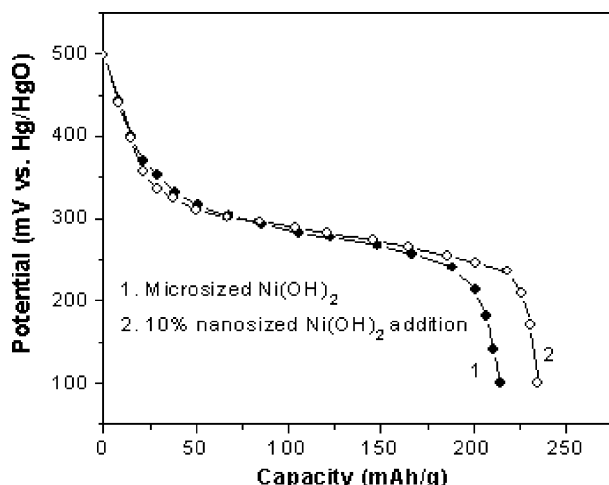
Fig. 9. Discharge curves for (a) the Ni(OH)$_2$ electrode with 10% nanosized Ni(OH)$_2$ addition and (b) microsized spherical Ni(OH)$_2$ electrode at a rate of 0.2 C.

Ni(OH)$_2$ addition exhibits a clearly increased discharge potential plateau region in Fig. 9, which is in good agreement with the above cyclic voltammetric experimental results. Based on the above analysis, it can be concluded that the Ni(OH)$_2$ electrode with 10% nanosized Ni(OH)$_2$ addition has excellent electrochemical properties in comparison with microsized Ni(OH)$_2$ electrode.

Usually common nickel hydroxide is spherical with a dimension of micrometer, and by definition, nanosized materials have at least one physical dimension less than 100 nm in length. When nanosized spherical Ni(OH)$_2$ is added to common microsized spherical Ni(OH)$_2$, it will be fully filled in the interspace of common spherical Ni(OH)$_2$ particles, which helps to enough contact and can shorten the route of proton diffusion among common microsized Ni(OH)$_2$ particles. Whilst, on the other hand, nanosized Ni(OH)$_2$ powder prepared by this method has a very small crystalline size and a large specific surface area, thus it shows a higher proton diffusion coefficient in comparison with microsized Ni(OH)$_2$ [3,10]. The both aspects accelerate the rate of proton diffusion in nickel hydroxide electrode. As we know that the step of proton diffusion is the rate-determining-step in nickel hydroxide electrode [11,12], the increase of the rate of proton diffusion means that the reaction activity of nickel hydroxide is enhanced, moreover contact between the active material and the electrolyte is enhanced, and results in the decrease of concentration polarization of electrode during charge–discharge process. Accordingly, the utilization of the active material of Ni(OH)$_2$ is improved and the Ni(OH)$_2$ electrode with 10% nanosized Ni(OH)$_2$ addition exhibits excellent electrochemical performance.

4. Conclusion

Nanosized spherical Ni(OH)$_2$ was prepared by the precipitate-transformation method. Characterization by XRD and TEM showed that it has a typical β(II)-phase structure with the particle size from 5 to 35 nm. Electrochemical measurements revealed that the Ni(OH)$_2$ electrode with 10% nanosized Ni(OH)$_2$ addition exhibits excellent electrochemical performance, e.g. smaller polarization and better discharge property than common microsized spherical Ni(OH)$_2$ electrode.

References

[1] M. Oshitani, H. Yufu, K. Takashima, S. Tsuju, J. Electrochem. Soc. 136 (1989) 1590.
[2] S.R. Ovshinsky, M.A. Fetcenko, J. Ross, Science 260 (1993) 176.
[3] K. Watannabe, T. Kikuoka, J. Appl. Electrochem. 25 (1995) 219.
[4] D.E. Reisner, A.J. Salkind, P.R. Strutt, T. Danny Xiao, J. Power Sources 65 (1997) 231.
[5] X. Han, X. Xie, C. Xu, D. Zhou, Y. Ma, Optical Mater. 23 (2003) 465.
[6] H.P. Klug, E.A. Leroy, X-ray Diffraction Procedure, Wiley, New York, 1974, p. 656.
[7] K. Nakamoto, Infrared Spectra of Inorganic and Coordination Compounds, Wiley, New York, 1963.
[8] R.M. Mallya, J. Indian Inst. Sci. 43 (1961) 148.
[9] M.J. Readey, R.R. Lee, J.W. Halloran, J. Am. Ceram. Soc. 73 (1990) 1499.
[10] Z. Zhou, J. Yan, J. Lin, Y.S. Zhang, Chin. J. Power Sources 23 (1999) 319 (in Chinese).
[11] R. Barnard, C.L. Randell, F.L. Tye, J. Appl. Electrochem. 10 (1980) 109.
[12] S. Motupally, C.C. Streiz, W.J. Weidner, J. Electrochem. Soc. 145 (1998) 29.